

## A New Technique to improve RFI suppression in Radio Interferometers

D. Anish Roshi

*National Radio Astronomy Observatory (NRAO), Box 2, Green Bank,  
 West Virginia 24944, USA*

R. A. Perley

*National Radio Astronomy Observatory (NRAO), P.O. Box O, 1003  
 Lopezville Road Socorro, NM 87801-0387*

**Abstract.** Radio interferometric observations are less susceptible to radio frequency interference (RFI) than single dish observations. This is primarily due to : (1) fringe-frequency averaging at the correlator output and (2) bandwidth decorrelation of broadband RFI. Here, we propose a new technique to improve RFI suppression of interferometers by replacing the fringe-frequency averaging process with a different filtering process. In the digital implementation of the correlator, such a filter should have cutoff frequencies  $< 10^{-6}$  times the frequency at which the baseband signals are sampled. We show that filters with such cutoff frequencies and attenuation  $> 40$  dB at frequencies above the cutoff frequency can be realized using multirate filtering techniques. Simulation of a two element interferometer system with correlator using multirate filters shows that the RFI suppression at the output of the correlator can be improved by 40 dB or more compared to correlators using a simple averaging process.

### 1. Introduction

Radio interferometers provide high-resolution, high-dynamic range radio images of celestial objects. It is well known that radio interferometers are less susceptible to radio frequency interference (RFI) compared to single dish. However, the dynamic range of the images in many cases is limited by interference indicating the need to improve RFI suppression.

In this paper, we describe a new technique to improve RFI suppression in interferometers <sup>1</sup>. The basic idea is to replace the averaging done at the output of the correlator with a multirate filtering process. A brief discussion of RFI suppression in existing interferometers is given in Sec. 2. Sec. 3 describes the proposed technique, gives the design of the multirate filter and presents simulation results. The limitations of the proposed technique are discussed in

---

<sup>1</sup>To our knowledge a technique similar to that discussed in this paper was used earlier in Mauritius Radio Telescope data reduction (Sachdev, Udayashankar 1995).

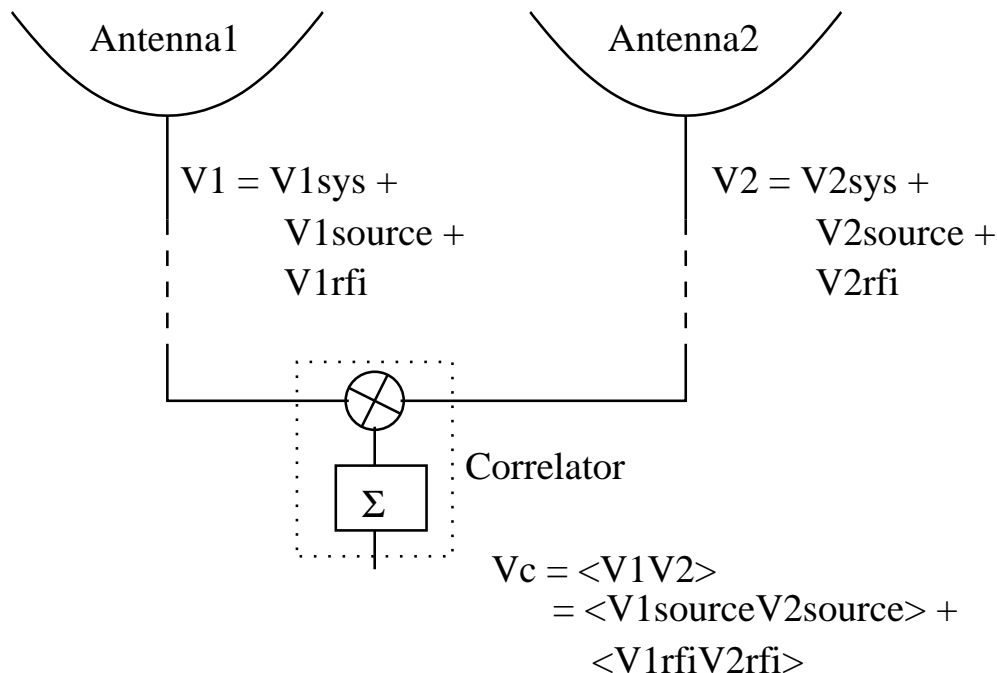


Figure 1. Schematic of a two element interferometer near an RFI source. The outputs of the antennas consists of the RFI ( $V_{1rfi}$ ,  $V_{2rfi}$ ), the system noise ( $V_{1sys}$ ,  $V_{2sys}$ ) and the source noise ( $V_{1source}$ ,  $V_{2source}$ ). Interferometers usually use a complex correlator to measure both amplitude and phase of the output of the correlator. Here, for simplicity, we consider the ‘real’ part of the complex correlator. The mean value of the correlator output will be the sum of the time averages of the product of the voltages due to the source and that due to the RFI.

Sec. 4 and the effects of the multirate filtering process in the visibility and spatial domain are discussed in Sec. 5.

## 2. RFI suppression in existing Radio Interferometers

### 2.1. Correlated and Uncorrelated RFI

In the case of interferometric observations interference can be broadly classified as correlated and uncorrelated RFI. Consider a two element interferometer near a RFI source (Fig. 1). The voltages  $V_1$  and  $V_2$  at the outputs of the two antennas each consists of three components — the system noise ( $V_{1sys}$ ,  $V_{2sys}$ ), the source noise<sup>2</sup> ( $V_{1source}$ ,  $V_{2source}$ ) and the RFI component ( $V_{1rfi}$ ,  $V_{2rfi}$ ). For the moment we will not consider fringe stopping, which is the case when the source is at the north pole. Also we consider that the RFI is not moving with respect to the interferometer. Interferometers usually use complex correlators,

<sup>2</sup>The source noise is that component of the sky noise which is not ‘resolved’.

which are constituted of ‘real’ and ‘imaginary’ parts. For the discussion in this paper, we consider a ‘real’ correlator. But the analysis is equally applicable to the ‘imaginary’ part of the correlator as well. The mean value of the correlator output,  $V_c$ , is given by

$$V_c = \langle V_1 V_2 \rangle = \langle V_{1source} V_{2source} \rangle + \langle V_{1rfi} V_{2rfi} \rangle, \quad (1)$$

where  $\langle \rangle$  denotes time average. If the separation between antennas (baseline length) is  $>$  a few 100 kms, which is the case for the VLBI (very long baseline interferometry), and if the RFI source is near one of the antennas, then the second antenna will not pick up the RFI (ie say  $V_{1rfi} = 0$ ). This means that  $V_c$  does not have any contribution from the RFI source or that the RFI is uncorrelated. If this condition is not true then the RFI is correlated (for this discussion we consider that the bandwidth of the system is very small so that there is no bandwidth decorrelation). In most connected interferometers RFI is correlated in many baselines. For the VLBI, most terrestrial RFI is uncorrelated, but satellite interference can be correlated in most ‘short’ baselines. The technique discussed in this paper to suppress interference deals with correlated RFI. Note that the RMS (root mean square) value of the correlator output is proportional to the geometric mean of the total powers at the inputs of the correlator if the source noise power is much smaller than the system noise power. The correlator input powers have contributions from the RFI even if it is uncorrelated. Thus uncorrelated RFI also limits the dynamic range of the image.

## 2.2. Fringe stopping and correlated RFI

For simplicity consider that the baseline of the two element interferometer is in the East-West direction. The output of the two antennas are connected to a correlator with cables of equal length (Fig. 2). The response of the interferometer  $P(\theta)$  is given by (Thompson, Moran, Swenson, 2001)

$$P(\theta) = P_{ant}(\theta) \cos\left(\frac{2\pi D \sin(\theta)}{\lambda}\right), \quad (2)$$

where  $P_{ant}(\theta)$  is the cross response of the two antennas,  $D$  is the baseline length and  $\lambda$  is the operating wavelength.  $\theta$  is measured with respect to the zenith, which we equate to the hour angle (HA) in radians for simplicity. A source moving through the interferometer response produces “fringes” at the output of the correlator. The fringe frequency  $f_{fringe}$  in the present case is given by,

$$f_{fringe} = \frac{D}{\lambda} \cos(HA) \frac{d(HA)}{dt} \cos(\delta), \quad (3)$$

where  $\delta$  is the declination of the source and  $\frac{d(HA)}{dt}$  is in units of radians per sec. The general equation for the fringe frequency is (Thompson et al. 2001)

$$f_{fringe} = \frac{d(HA)}{dt} u \cos(\delta), \quad (4)$$

where  $u$  is the projected baseline in the East-West direction in units of  $\lambda$ . The above equation shows that the fringe frequency due to a source depends on

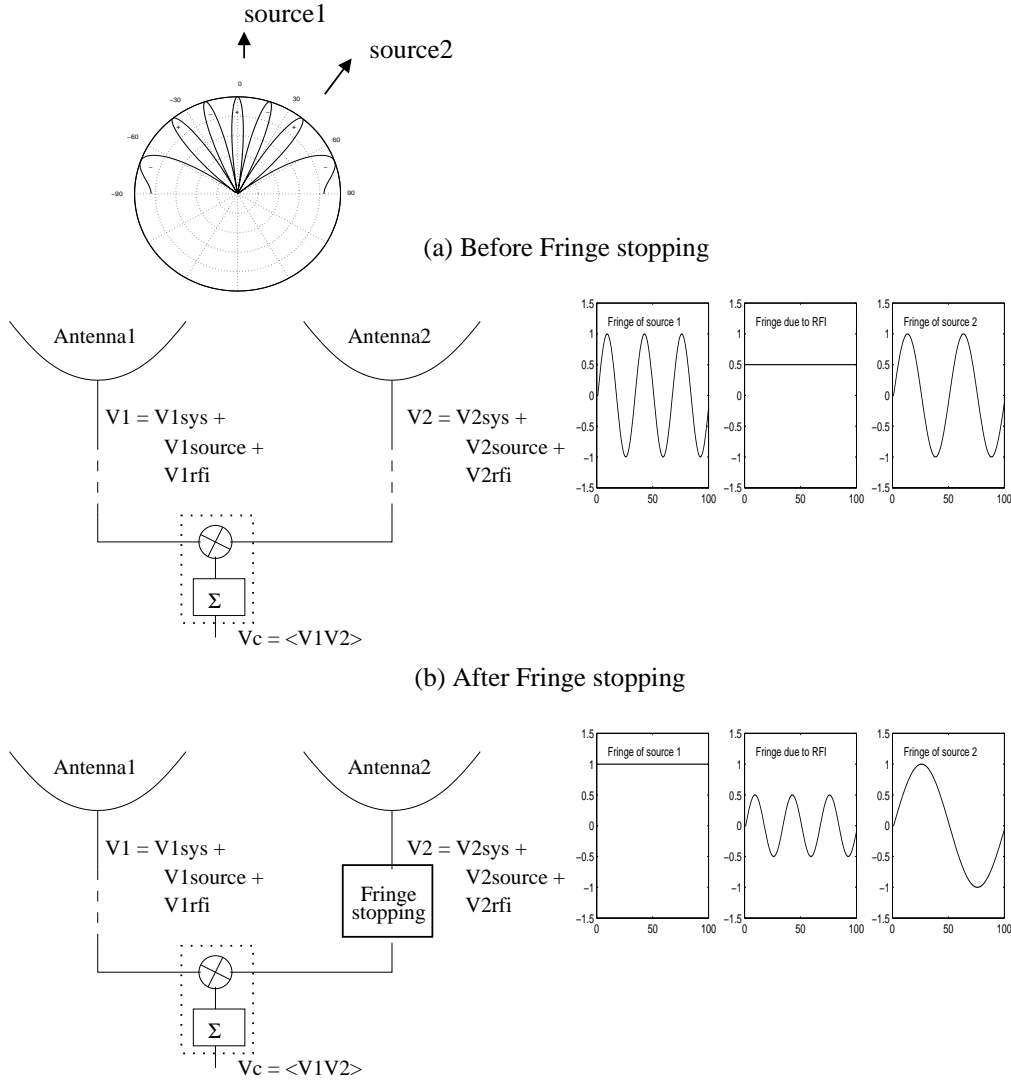


Figure 2. Schematic showing the effect of fringe stopping in a two element interferometer. The response of the two element interferometer is shown on the top in polar diagram. If no fringe stopping is done the source moves through this response producing a fringe at the output of the correlator. The fringe frequency due to sources separated in sky are different which is schematically shown in figure (a). The RFI power at the output of the correlator in this case will be constant. After fringe stopping, as shown in figure (b), the component of the correlator output due to the source at the phase center (source 1 in figure) will be constant and the RFI will produce a fringe. A source away from the phase center (source 2) will still produce a fringe but its frequency will be the difference between its original fringe frequency and the fringe stopping frequency. The figure represents the case when either the RFI is narrow band or the spectral resolution of the receiver system is less than the differential fringe frequency.

the projected baseline and earth's rotation rate ( $= \frac{d(HA)}{dt}$ ). Now consider a terrestrial, stationary, correlated RFI. Since the position of the RFI does not change with respect to the interferometer, there will be no fringe due to the interference.

For observations with the interferometer, the interferometer is 'phased' in the direction of the interested radio source through out the observations. This process of phasing the interferometer (which includes both delay compensation and fractional phase compensation) is called 'fringe stopping'. Fringe stopping essentially makes the correlator output constant due to a (point) source at the phase center. Sources away from the phase center produce fringes with frequencies equal to the difference between  $f_{fringe}$  of the source at the phase center and that of the source away from the phase center. Thus, in the above case, larger the difference between the  $HA$  of a source and that at the phase center the larger will be its 'differential' fringe frequency. This also means that the correlated RFI now produces a fringe with a frequency equal to  $f_{fringe}$  of the source at the phase center because of fringe stopping.

### 2.3. Fringe averaging and RFI suppression

Usually in interferometric observations, one is interested in mapping sources within the primary beam of the antenna. Typically the differential fringe frequencies due to these sources is much smaller than  $f_{fringe}$  of the source at the phase center. The maximum differential fringe rate is given by

$$\Delta f_{fringe} \sim \frac{d(HA)}{dt} \frac{\Omega_{antenna}}{\Omega_{synth}} \sim \frac{d(HA)}{dt} \frac{D}{D_{antenna}}, \quad (5)$$

where  $\Omega_{antenna}$  and  $D_{antenna}$  are the beam and diameter of each element of an interferometer,  $\Omega_{synth} \sim \lambda/D$  is the synthesized beam,  $\lambda$  is the operating wavelength and  $D$  is the baseline length. Consider, for example,  $D = 10$  km and  $D_{antenna} = 25$  m. The differential fringe frequency is  $\sim 0.005$  Hz while  $f_{fringe}$  of the source at the phase center is  $\sim 3.5$  Hz, for  $\lambda = 0.21$  m. The low differential fringe frequency allows one to average the output of the correlator for several seconds. Since the RFI produces a fringe (due to fringe stopping process) this averaging reduces the amplitude of the RFI at the correlator output thus making the interferometer less susceptible to RFI (see Perley 2002 for a quantitative estimate of RFI attenuation in Very Large Array due to fringe averaging). An additional suppression of broadband RFI occurs due to bandwidth decorrelation, which is a bonus over the former effect. We will not discuss the bandwidth decorrelation effect any further here (see Thompson et al. 2001).

### 3. A new technique to improve RFI suppression in Interferometers

The averaging at the correlator output can be thought of as a moving average filtering process. The response of such a filter is shown in Fig. 4. The stop-band attenuation (i.e. the attenuation of frequencies beyond the cutoff frequency) of the filter determines the amount of RFI suppression achieved in this process if the fringe due to RFI is beyond the cutoff frequency of the filter. As seen from Fig. 4, stop-band attenuation in the worst case is 13.5 dB. We propose that

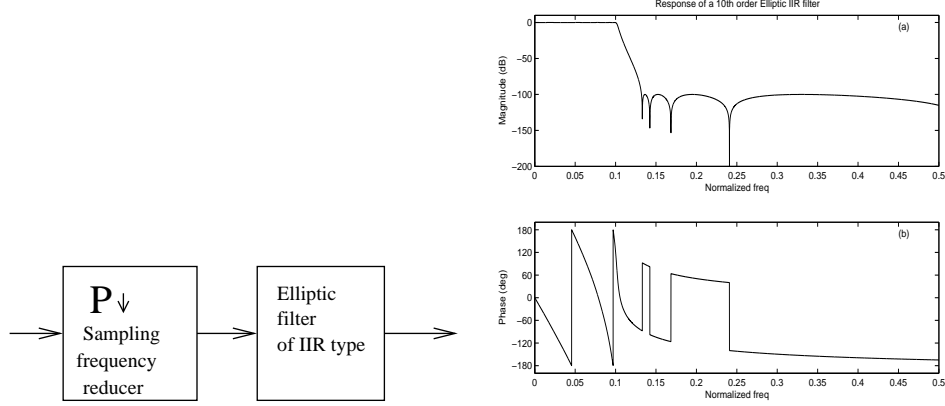


Figure 3. Block diagram of a multirate filter (left). The first block reduces the sampling frequency. The basic filter that needs to be implemented follows the resampling block, which is a digital elliptic filter in our design. The amplitude and phase response of the elliptic filter is shown on right.

RFI suppression in interferometers can be improved by using a filter with high stop-band attenuation at the output of the correlator. In the following sections we show how such filters can be designed and present results of the simulation done to test its performance.

### 3.1. Multirate filtering

Present day correlators are designed using digital techniques. The typical bandwidth of the interferometer is a few tens of MHz or more. Sampling the signals at Nyquist rate implies that the data rate at the output of the multiplier will be of the order of the bandwidth. As mentioned above the output of the correlator can be averaged for several secs. This means that the required cutoff frequency of the filter that replaces the simple averaging should be a few tenths of a Hz. Thus the normalized (normalized with half the Nyquist frequency of the baseband) cutoff frequency of the filter is  $< 10^{-6}$ . A direct realization of a digital filter is not practical in such situations. However, such filters are realizable using multirate filtering technique. This technique essentially implements the required filter after reducing the sampling frequency (see Fig. 3; Bellanger 2000).

The basic filter used for the multirate filtering design is a digital elliptic filter. Using Matlab, a digital elliptic filter of order 10 with normalized cutoff frequency of 0.1 and stopband attenuation of 100 dB is designed. The passband ripple is chosen as 0.1 dB. The elliptic filter is realized using IIR (infinite impulse response) filter sections and its response is shown in Fig. 3. The sampling rate reduction is done in two ways: (1) using polyphase filtering technique; (2) by low-pass filtering the data using a moving average filter and then resampling the data at half the number of points averaged. The second type of filter is economical and simpler to implement in hardware. For testing the performance of the filter the sampling rate is reduced by 100. Thus the effective cutoff frequency of the filter is  $10^{-3}$  and we believe that this could be scaled further

down by appropriately resampling the data. The responses of the multirate filters are shown in Fig. 4.

### 3.2. Results of the simulation

A simulation was done in Matlab to determine the improvement in RFI rejection of a two element interferometer by implementing the multirate filtering process. Fig. 5 shows the block diagram of the interferometer implemented for the simulation. The fringe generator adds a fringe to the source noise. The antenna blocks are power combiners, combining the source noise, the two independent system noises and the RFI. All noises are Gaussian random variables. The response of the receiver is realized using the receiver filters. Fringe stopping is done before multiplying the two antenna outputs. The relative delay between the two antennas is made Zero for the simulation.

The designed multirate filters and the moving average filter are used as post-detection filters to study their relative performance. A sine wave with normalized frequency of 0.65 is used as RFI. The receiver bandwidth in normalized frequency is selected as 0.2 centered at 0.625. The receiver noise ( $T_{sys}$ ) and source noise powers are made equal to 0.2 in arbitrary units. Fig. 6 shows the spectra of the two receiver outputs. The source noise is multiplied with a fringe of normalized frequency  $3 \times 10^{-3}$ . If we consider that this fringe freq should translate to say 3 Hz, then the Nyquist frequency will be 2.0 KHz. This choice of the fringe frequency is limited by the practicality of the simulation. The outputs of the correlator for different types of post-detection filters are shown in Fig. 7. The remarkable ( $> 40$  dB) improvement in the RFI suppression compared to the case when a moving average filter is used as post-detection filter is evident from this figure. Comparing the spectrum of the correlator output with a moving average post-detection filter and multirate post-detection filter shows that the spectral values below the cutoff freq of the filter are almost the same for both cases. This means that the amplitudes of the desired fringe frequencies are not affected by the multirate filtering process.

The effectiveness of the technique is also determined by estimating the spectral power of the RFI at the output of the correlator with different types of post-correlation filters. To estimate the spectral power of RFI a power spectrum of the correlator output is first made. The difference of the spectral values of the channels where the RFI is expected and the average of the values of the two nearby channels is then taken. If the RFI power is comparable to the noise fluctuations in the spectrum then the difference can also be negative. We assigned a value of zero for the RFI spectral power if the estimate is negative. Fig. 6 shows the spectral power of RFI vs the interference-to-noise ratio (INR) of the RFI at the output of the receiver. The INR is the ratio of the RFI power to the noise power (receiver noise + source noise) at the output of the receiver. The remarkable suppression of the spectral power of the RFI with a multirate filter in post-detection stage is clear from Fig. 6.

### 4. Limitations of the technique

The technique discussed in this paper to improve RFI suppression of interferometers is effective only for correlated RFI (see Sec. 2). Usually terrestrial RFI is

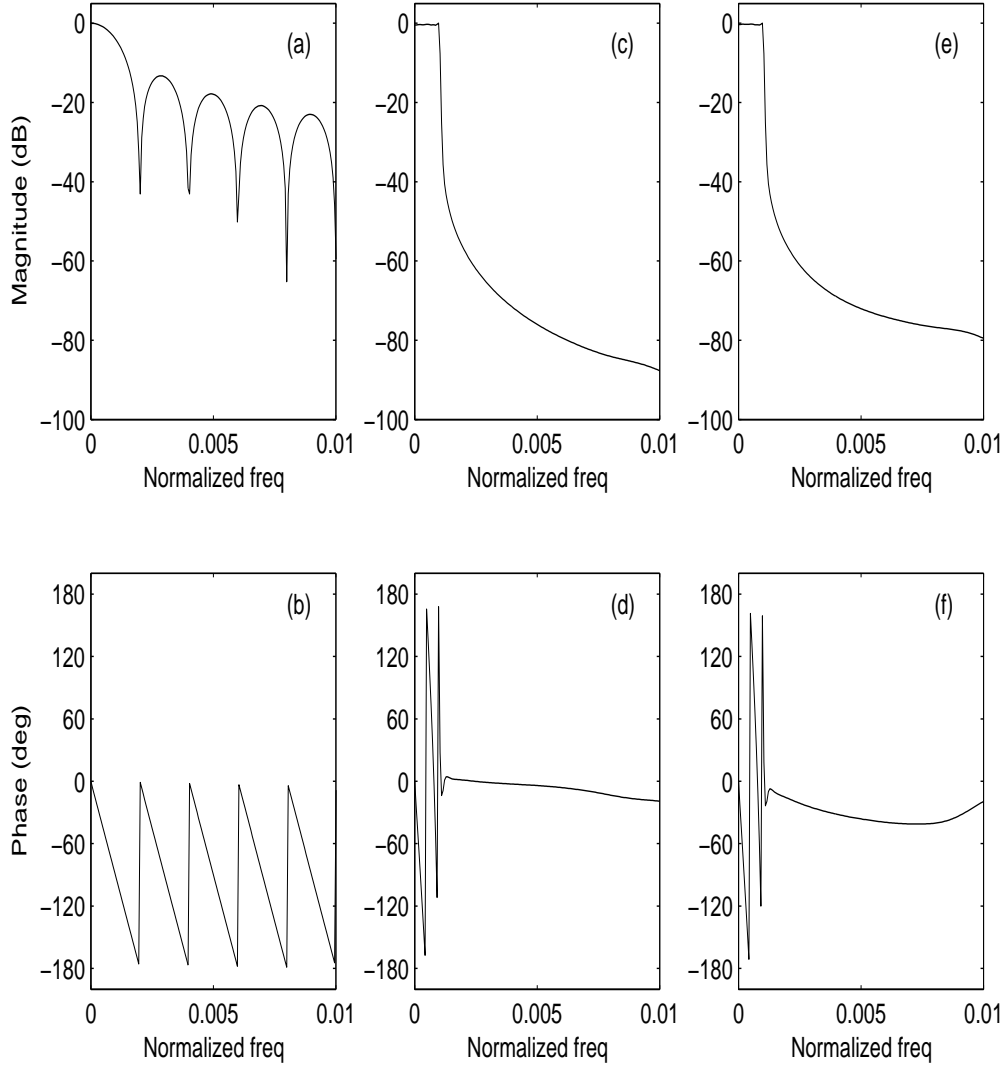


Figure 4. Multirate filter responses along with that of a moving average filter. The amplitude and phase response of a 1000 point moving average filter is shown in (a) & (b). Response of a multirate filter with resampling done using polyphase filtering followed by a digital elliptic filter is shown in figure (c) & (d). Figs. (e) & (f) shows the response of a multirate filter with a moving average filter followed by an elliptic filter. (See text for details).



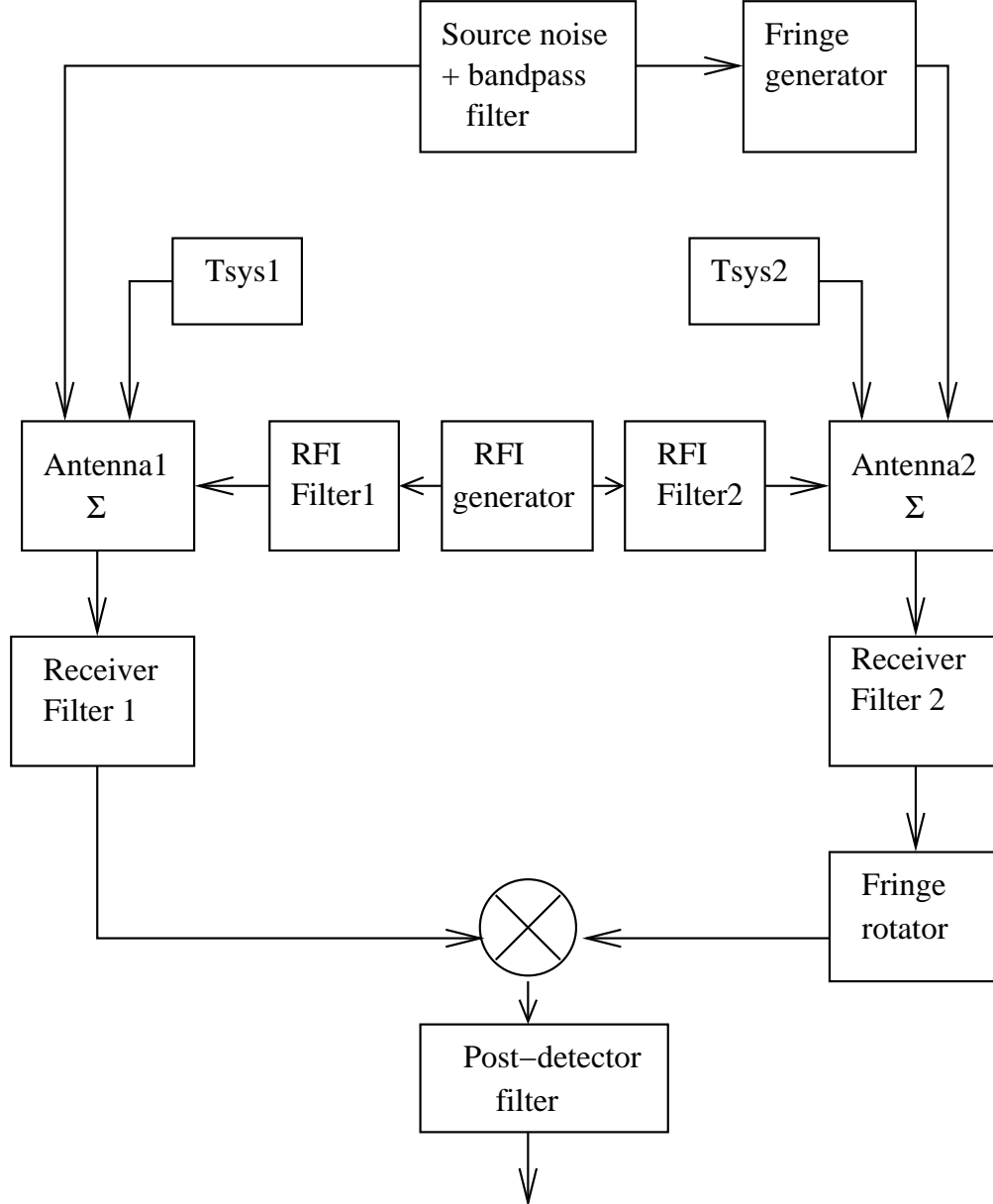


Figure 5. Block diagram of the two element interferometer used for the simulation. The fringe generator introduces a fringe in the source noise and the fringe rotator block does the ‘fringe stopping’. A moving average filter and two types of multirate filters are used as post-detection filters (see Sec. 3) to determine their relative performance in suppressing RFI.

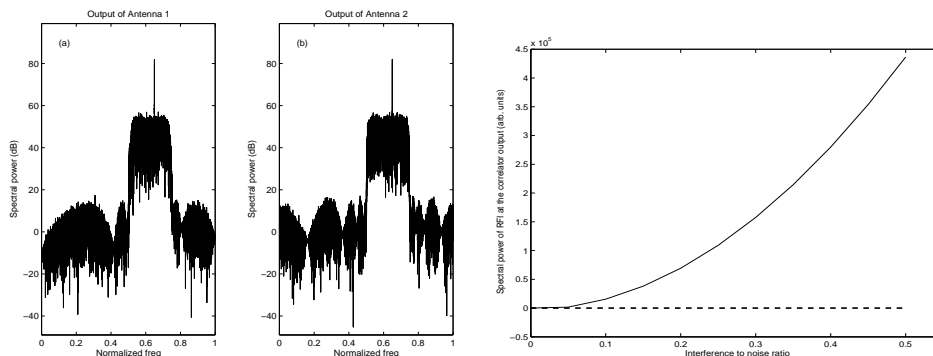


Figure 6. Spectra of the outputs of the antennas obtained in the simulation is shown on left. The RFI is located at 0.65. The spectral power of the RFI at the output of the correlator against the interference-to-noise ratio at the antenna output is plotted on right. The data with a moving average post-detection filter is shown in solid curve. The dashed line corresponds to the data with multirate filter using polyphase technique as post-detection filter.

correlated on baselines of length less than a few 100 kms. Correlated RFI produces fringes at the output of the interferometer. The fringe frequency depends on the baseline length as well as the source declination for a given hour angle. Effective suppression of RFI occurs if the fringe frequency is much above the cut-off frequency of the multirate post-detection filter (see Sec. 3). However, if the baselines are small ( $<$  a few kms) then the fringe frequency will be small and it becomes difficult to make filters that can attenuate these frequencies. Thus the technique presented here gives good RFI rejection for intermediate ( $\sim$  a few kms to a few 100 kms) baselines. The fringe frequency also becomes smaller for sources near the north celestial pole (declinations near  $90^\circ$ ), which means that this technique will not work efficiently for this case as well.

Often RFI will have a strong carrier and associated modulating frequency components. The modulation results in a wider spectrum of the RFI at the output of the correlator. Thus only those components below the cut-off frequency of the multirate filter will be attenuated.

The analysis and simulation presented in this paper consider that the RFI is not time variable. However, in reality RFI is time variable. The response of the multirate filter to transient RFI needs to be studied. This will be presented elsewhere.

## 5. Effects of multirate filtering on the visibility and spatial domain

Till now the effect of the multirate filtering technique is discussed in relation with the time series at the output of the correlator. Any processing of the correlator output has an equivalent effect on the visibility domain and correspondingly on the spatial domain (i.e. positions in sky). The effective position of a stationary RFI is the north celestial pole. Thus suppressing the RFI using the multirate

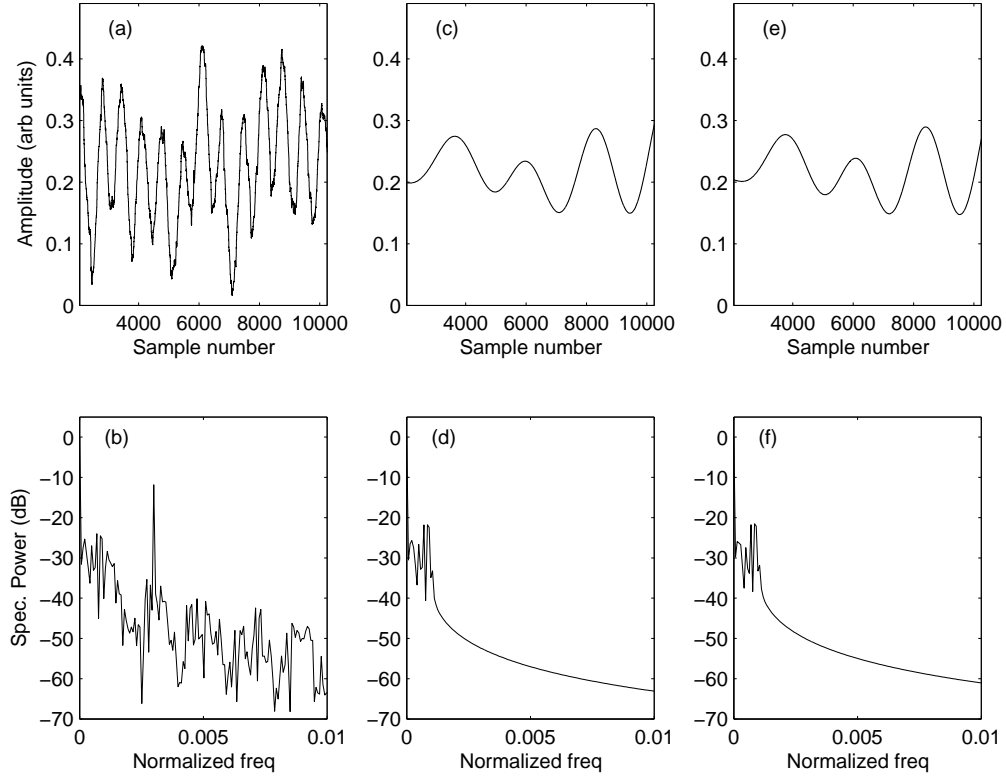


Figure 7. Time series of the correlator output and its spectrum. Figs (a) & (b) are obtained with a moving average post-detection filter. A multirate filter which uses polyphase filter to resample the data is used as the post-detection filter to get Figs (c) & (d). Figs (e) & (f) are obtained using a multirate filter which uses a moving average filter to resample the data.

filtering process is equivalent to introducing a spatial null at the north celestial pole. In fact, the spatial null is not confined to the north celestial pole alone but extends along the spatial domain where the differential fringe frequencies are larger than the cutoff frequency of the multirate filter. The attenuation due to the spatial null will be proportional to the attenuation of the RFI due to the multirate filter.

In the visibility domain, the multirate filtering process essentially convolves the true visibility with the filter response along  $uv$  tracks traced by pairs of antennas in an interferometer. Depending on the filter response, the amplitude and phase of the spatial frequencies of interest are modified. Since the filter is implemented digitally its response is known well and is identical for all the correlators. With the knowledge of this filter response, we believe a correction similar to the primary beam correction can be done to take out the effect of filtering. A detailed discussion on this will be presented elsewhere.

## **6. Acknowledgment**

DAR thanks Rick Fisher for all useful discussions during the course of this work. The basic idea described in this paper stemmed from a discussion DAR had with Prof. A. Pramesh Rao, National Center For Radio Astrophysics, Pune, India.

## **References**

- Bellanger, M., 2000, Digital Processing of Signals, John Wiley & Sons, Ltd, Chichester, UK.
- Perley, R., 2002, EVLA Memo No. 49, NRAO Library, Socorro.
- Sachdev, S., Udayashankar, N., 1995, BASI, 23, 574.
- Thompson, A. R., Moran, J. M., Swenson, Jr., G. W., 2001, Interferometry and Synthesis Technique, John Wiley & sons, inc., New York.